Natural Resistance to Intracellular Infections: Natural Resistance–associated Macrophage Protein 1 (NRAMP1) Functions as a pH-dependent Manganese Transporter at the Phagosomal Membrane

By Nada Jabado,* Andrzej Jankowski,‡ Samuel Dougaparsad,‡ Virginie Picard,* Sergio Grinstein,‡ and Philippe Gros*

*From the *Department of Biochemistry, McGill University, Montreal H3G-1Y6, Quebec, Canada; and the ‡Division of Cellular Biology, The Hospital for Sick Children, Toronto M5G 1X8, Ontario, Canada*

Abstract

Mutations at the natural resistance–associated macrophage protein 1 (*Nramp1*) locus cause susceptibility to infection with antigenically unrelated intracellular pathogens. *Nramp1* codes for an integral membrane protein expressed in the lysosomal compartment of macrophages, and is recruited to the membrane of phagosomes soon after the completion of phagocytosis. To define whether Nramp1 functions as a transporter at the phagosomal membrane, a divalent cation-sensitive fluorescent probe was designed and covalently attached to a porous particle. The resulting conjugate, zymosan–FF6, was ingested by macrophages and its fluorescence emission was recorded in situ after phagocytosis, using digital imaging. Quenching of the probe by Mn^{2+} was used to monitor the flux of divalent cations across the phagosomal membrane in peritoneal macrophages obtained from Nramp1-expressing (+/+) and Nramp1-deficient (−/−) macrophages. Phagosomes from $Nramp1^{+/+}$ mice extrude Mn^{2+} faster than their $Nramp^{-/-}$ counterparts. The difference in the rate of transport is eliminated when acidification of the phagosomal lumen is dissipated, suggesting that divalent metal transport through Nramp1 is H^+ dependent. These studies suggest that Nramp1 contributes to defense against infection by extrusion of divalent cations from the phagosomal space. Such cations are likely essential for microbial function and their removal from the phagosomal microenvironment impairs pathogenesis, resulting in enhanced bacteriostasis or bactericidal activity.

Key words: Nramp1 • transporter • divalent cation • phagosome • V-ATPase

Introduction

A better understanding of natural host defenses against infections may provide alternative strategies for intervention to combat the emerging strains of drug-resistant microbes. In mice, the *Bcg/Ity/Lsh* locus on chromosome 1 dictates differential susceptibility to infection with a variety of antigenically unrelated intracellular pathogens by modulating the capacity of the macrophage to restrict their intracellular replication (for reviews, see references 1 and 2). Natural resistance–associated macrophage protein 1 (*Nramp1*)[1] was isolated by positional cloning of *Bcg/Ity/Lsh* (3), and it was subsequently shown that naturally occurring (4) or experimentally induced (5) loss of function mutations at *Nramp1* cause susceptibility to infection with several species of *Mycobacterium*, *Salmonella,* and *Leishmania* (5). In addition, polymorphic variants at human *NRAMP1* have been found to be associated with susceptibility to tuberculosis (6, 7) and leprosy (8) in endemic areas of disease. Also, a recent linkage study performed in an outbreak situation shows a strong linkage between susceptibility to tuberculosis and haplotypes of human *NRAMP1* (9). However, other studies have failed to detect an association between *NRAMP1* and susceptibility to infections (10). *Nramp1* mRNA is expressed primarily in macrophages and polymorphonuclear leukocytes (3, 11, 12) and is upregulated in these cells by exposure to activating or inflammatory stimuli (11). The pleiotropic effect of *Nramp1* mutations on host susceptibil-

Address correspondence to Philippe Gros, Department of Biochemistry, McGill University, 3655 Drummond St., Montreal H3G-1Y6, Quebec, Canada. Phone: 514-398-7291; Fax: 514-398-2603; E-mail: gros@med.mcgill.ca

[1]*Abbreviations used in this paper:* Nramp1, natural resistance–associated macrophage protein 1; TM, transmembrane.

ity to multiple intracellular infections, together with the restricted expression of *Nramp1* mRNA to professional phagocytes, suggests that Nramp1 protein plays a key role in the antimicrobial function of these cells.

Nramp1 is a highly hydrophobic integral membrane phosphoglycoprotein of ~100 kD (13). Its primary sequence suggests the presence of 12 transmembrane (TM) domains that contain a total of 9 charged residues. These polar residues impart an amphipathic character to several TM segments, as found in TM helices of several ion transporters and channels (14, 15). Nramp1 also contains the "consensus transport motif" detected in several prokaryotic and eukaryotic membrane transporters (14). Immunolocalization studies indicate that Nramp1 is expressed in the late endosomal/early lysosomal compartment of the cell, where it colocalizes with the lysosomal marker lysosomal-associated membrane protein 1 (Lamp1; 16, 17). Immunofluorescence analyses and biochemical studies have demonstrated that upon phagocytosis of inert particles or live bacteria, Nramp1 is rapidly recruited to the membrane of phagosomes, where it remains associated during maturation to phagolysosomes (16, 18). Targeting of Nramp1 to the phagosomal membrane has a major effect on the physiological properties of this vacuole; indeed, Nramp1-positive mycobacterial phagosomes show enhanced fusion to vacuolar H^+-ATPase–positive vesicles (19) and to lysosomes (20), increased acidification (19), and enhanced bactericidal activity (18) compared with their Nramp1-negative counterpart.

The mechanism whereby Nramp1 contributes to the antimicrobial activity of macrophages and the possible substrate transported at the phagosomal membrane remain poorly understood. However, the characterization of Nramp homologues from other organisms has provided important clues. Indeed, the primary and secondary structures of members of the family defined by Nramp1 have been highly conserved throughout evolution, from bacteria to humans (14, 15). The close mammalian homologue, Nramp2 (also known as DCT1 [21] and DMT1 [22]), shares 78% amino acid identity in the hydrophobic core with Nramp1. It is expressed ubiquitously (23) and is found at the plasma membrane, as well as in early (24) and late endosomes (25) of several cell types. Nramp2 is present at the brush border of the duodenum, where its expression is regulated by dietary iron (26). Functional analyses in *Xenopus* oocytes have shown that Nramp2 functions as a pH-dependent divalent cation transporter (21). The *Nramp2* gene is mutated (G185R) in two rodent models of iron deficiency, the mk mouse and the Belgrade rat, both of which present impaired intestinal iron uptake and severe microcytic anemia (27, 28). Thus, Nramp2 is the major transferrin-independent iron uptake system of the mammalian intestine. Likewise, the yeast *smf1* homologue (40% identity) is a divalent cation transporter (29, 30), and mouse *Nramp2* can functionally complement a yeast *smf1/smf2* mutant (31). In addition, mutations in the fly *Nramp* homologue, *malvolio*, cause a taste discrimination defect that can be suppressed by supplementing flies with dietary divalent metals, or expressing a human *Nramp1* gene in transgenic *malvolio* flies (32, 33). Finally, *Nramp* homologues have been identified in several bacterial species, and the *Mycobacterium tuberculosis* (34) and *Escherichia coli* homologues (35) have been functionally characterized as divalent cation transporters.

The high degree of sequence similarity between Nramp1 and Nramp2, together with the conservation of function in the Nramp superfamily, suggests that Nramp1 may also function as a divalent cation transporter. However, the possible role of Nramp1 as a transporter has been difficult to establish experimentally. This is likely because Nramp1 is exclusively localized in endomembrane compartments that are not readily accessible for transport assays. Attempts to define Nramp1 function using radioisotopes and fluid-phase fluorescent indicators have produced contradictory results (36–38). The difficulty in distinguishing bound from transported isotope and the possible damage incurred in the purification of isolated macrophages may have contributed to this ambiguity.

We have devised an approach to measure fluxes of divalent cations across the membrane of phagosomes in situ by noninvasive spectroscopic means. To this end, we designed a divalent cation-sensitive fluorescent probe that was covalently coupled to particles that could be opsonized and internalized by macrophages. Microfluorescence imaging of intact macrophages that had ingested this probe was used to monitor the effect of Nramp1 recruitment on divalent cation fluxes across the phagosomal membrane.

Materials and Methods

Materials. Thapsigargin and concanamycin were purchased from Calbiochem-Novabiochem. *N*,*N*,*N*′,*N*′-tetrakis 2-pyrimethylethylenediamine (TPEN) was obtained from Sigma-Aldrich. Fura-2 acetoxymethyl ester was from Molecular Probes. Diphenylene iodonium was synthesized in our laboratory according to a method described previously (39). The polyclonal rabbit anti-Nramp1 antiserum was raised and affinity purified as described previously (16).

Preparation of Zymosan–FF6 Particles. The strategy used to synthesize the particulate fluorescent probe zymosan–FF6 is shown in Fig. 1. The precursor, Fura-6-FF-tetraethylester (COOH-FF6[COOEt]$_4$), was purchased from TeFLabs. COOH-FF6 (COOEt)$_4$ has four cation-sensitive carboxyl groups that are protected by esterification, with a fifth unprotected carboxylate that is used to covalently couple the precursor to amino groups on zymosan by carbodiimide-mediated activation using a succinimidyl ester. After attachment to the particles, the protecting ethyl ester moieties were removed by treatment with trimethylsilanoate.

For activation (step a in Fig. 1), 2.1 mg of COOH-FF6(COOEt)$_4$, 1 mg of dicyclohexylcarbodiimide, 1.8 mg of *N*-hydroxysuccinimide, and catalytic amounts of dimethyl amino pyridine were dissolved in 30 μl of anhydrous dimethyl formamide (all reagents from Sigma-Aldrich). The mixture was incubated overnight at room temperature in the dark in an orbital shaker, yielding NHS-FF6(COOEt)$_4$, which remained in solution, as well as an insoluble precipitate of dicyclohexylurea. The crude NHS-FF6(COOEt)$_4$ was used immediately and without further purification for coupling with zymosan (step b in Fig. 1).

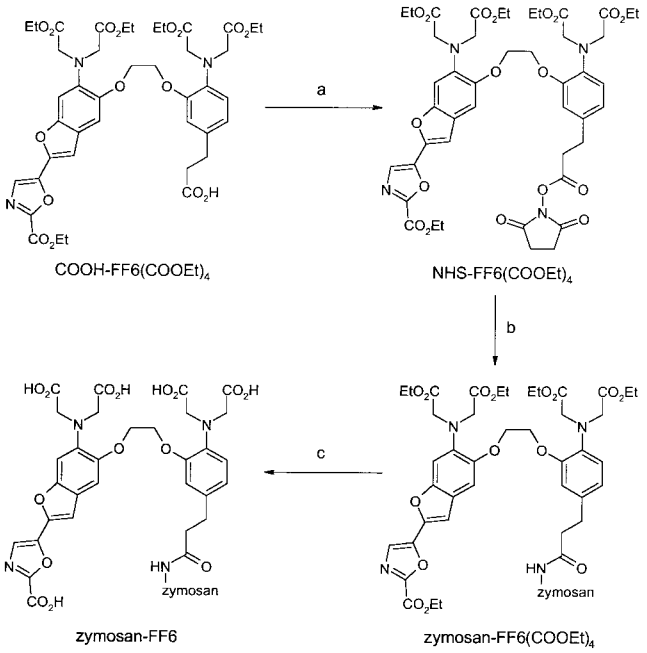

Figure 1. Synthesis of the fluorescent probe zymosan–FF6. Step a, activation of COOH-FF6$(COOEt)_4$ using dicyclohexylcarbodiimide and *N*-hydroxysuccinimide. Step b, coupling of the activated intermediate to zymosan. Step c, deprotection of the conjugate by silanolate-induced ester hydrolysis.

Coupling was accomplished by adding 30 μl dropwise of the NHS-FF6$(COOEt)_4$ solution to 25 mg of zymosan (Molecular Probes) suspended in 500 μl of 0.1 M sodium carbonate buffer, pH 8.5, with constant stirring. This mixture was stirred at 37°C for 4–5 h in the dark. The resulting labeled particles (zymosan–FF6$[COOEt]_4$) were recovered by centrifugation and washed with anhydrous dimethyl sulfoxide (Sigma-Aldrich) until removal of free NHS-FF6$(COOEt)_4$, monitored as disappearance of fluorescence from the supernatant, was complete. Carboxyl deprotection of zymosan–FF6$(COOEt)_4$ (step c in Fig. 1) was performed by resuspending 20 mg of potassium silanolate in 100 μl of anhydrous tetrahydrofuran, followed by the addition of 20 μl of 70% ethanol and the dropwise addition of 100 μl of the zymosan–FF6$(COOEt)_4$ suspension, followed by incubation at room temperature for 5 min. The resulting deprotected product, called zymosan–FF6 hereafter, was washed extensively with PBS before use.

Incubation Media. RPMI 1640 was purchased from Sigma-Aldrich. FCS was from GIBCO BRL. PBS consisted of 140 mM sodium chloride, 10 mM potassium chloride, 8 mM sodium phosphate, and 2 mM potassium phosphate, pH 7.4. Extracellular medium is a sodium-rich solution consisting of 140 mM NaCl, 3 mM KCl, 10 mM glucose, 20 mM Hepes, and 250 μM EGTA, without Ca^{2+} or Mg^{2+} and titrated to pH 7.3. Potassium-rich media contained 143 mM KCl, 1 mM $MgCl_2$, 10 mM glucose, and 20 mM Hepes, and were titrated to pH 7.5, 6.5, 5.5, 4.5, or 4, as indicated. In all cases, osmolarity was adjusted to 290 ± 5 mosM.

Cell Isolation. 129sv mice expressing a wild-type allele at the *Nramp1* locus (+/+) were originally obtained from Taconic Farms and subsequently maintained as a breeding colony, according to regulations of the Canadian Council of Animal Care. Mutant mice bearing a null mutation at the *Nramp1* locus (*Nramp1*$^{-/-}$) were produced by homologous recombination, as described previously (5). Resident peritoneal macrophages were obtained from 6–8-wk-old wild-type (+/+) and knockout (−/−) mice by peritoneal lavage with 10 ml of sterile PBS, as described (11). The harvested cell suspension contained ~30% mature macrophages as determined by Wright staining. Cells were washed twice with PBS and resuspended in RPMI 1640 containing 10% serum, 5 mM glutamine, and antibiotics (streptomycin and penicillin) before plating (10^6 cells/ml) on glass coverslips. 2 h later, nonadherent cells were removed by washing with fresh medium, and macrophages were used either immediately or 48 h later for phagocytosis and fluorescence imaging.

Immunofluorescence. Zymosan particles were prepared as follows: they were preswollen in PBS for 30 min at 20°C, followed by two additional washes in PBS. Macrophages were allowed to ingest zymosan particles for 30 min at 37°C and then washed extensively in ice-cold PBS before processing for immunofluorescence. Nramp1 was detected as described previously (16) with the following modifications: incubation with the affinity-purified anti-Nramp1 antiserum (1:150) was for 4 h at 20°C, followed by a 1-h incubation with a rhodamine-conjugated, goat anti–rabbit secondary antibody (1:300; Jackson ImmunoResearch Laboratories). Cells were examined using a ZEISS laser confocal microscope with a 63× objective, and composites of confocal images were assembled.

Spectrofluorimetry and Microfluorescence Imaging. The spectral properties of zymosan–FF6 particles (10 μl packed particles) were determined in a Hitachi F-4000 spectrofluorimeter using a thermostatted cuvette holder with magnetic stirring. For microfluorescence imaging, macrophages from wild-type (+/+) and *Nramp1* mutant mice (−/−) were plated on glass coverslips and incubated for 48 h. They were washed twice and overlaid with 1 ml of Na-rich medium containing 10 μM diphenylene iodonium and 10 μl of zymosan–FF6 suspension, followed by a further 30-min incubation at 37°C. The cells were next washed twice and coverslips were placed in a thermostatted Leiden holder on the stage of a Leica fluorescence microscope equipped with an HCX APO 100× oil immersion objective, which has high UV transmittance. A Sutter filter wheel positioned the excitation filter (360BP10 nm) in front of a mercury lamp. To minimize dye bleaching and photodynamic damage, a neutral density filter was used to reduce the intensity of the excitation light reaching the cells and each exposure was limited to 200 ms. The sample was continuously illuminated at >620 nm by placing a red filter in front of the incandescent source. By placing an additional 660-nm dichroic mirror in the light path, the red light was directed to a video camera allowing continuous visualization of cell morphology by Nomarski microscopy. Emitted light was selected through a 535BP25 nm filter placed in front of a cooled charge-coupled device camera (Princeton Instruments Inc.). Image acquisition was controlled by the Metafluor software (Universal Imaging Corp.) operating on an Intel Pentium II computer.

Measurement of Phagosomal pH. Measurements of phagosomal pH were obtained by fluorescence ratio imaging as described in the previous section, with the following modifications. In brief, cells were incubated with zymosan particles covalently labeled with both fluorescein and Oregon green 514 in the presence of 10 μM diphenylene iodonium for 30 min at 37°C. Excitation was alternated at 440 and 490 nm using the Sutter filter wheel and directed to the cells by a dichroic mirror (510 nm). Emitted fluorescence was selected through a 535BP25 nm filter and captured with the cooled camera.

Calibration of the fluorescence ratio versus pH was performed in situ for each experiment by equilibrating the cells in isotonic

K^+-rich medium buffered to predetermined pH values (between 7.5 and 4) after a 1-min permeabilization with 0.1% Triton X-100. Calibration with Triton X-100 yielded results similar to those obtained with protonophores, but was considerably faster. Calibration curves were constructed by plotting the extracellular pH, identical to the phagosomal pH under these conditions, against the corresponding fluorescence ratio.

Statistical Analysis. Data were treated by means of Statistic Analysis System (SAS) statistical package for computer analysis. Significant differences were declared if the *P* value for the F-statistic was ≤ 0.05.

Results

A noninvasive procedure was devised to study the possible role of Nramp1 in transporting cations across the phagosomal membrane. Our strategy was based on the use of a divalent cation-sensitive fluorophore that was targeted to the phagosome and maintained therein by covalent linkage to solid particles. Initial attempts to target fluorophores to the phagolysosome by uptake of probes present in the fluid phase were unsuccessful, due to quenching of the concentrated soluble probe and because the probe was widely distributed in the endocytic pathway. Likewise, efforts to use covalently derived latex particles resulted in failure because of the limited capacity of the beads, which expose reactive groups only on their outer surface. Thus, we opted for zymosan particles as a source of particulate, porous, and water-filled particles to which a sizable quantity of a cation-sensitive fluorophore could be coupled. The emission of individual internalized particles could then be monitored in real time within intact cells by microfluorescence imaging.

Characterization of Zymosan–FF6. Zymosan–FF6 was generated by covalently attaching the divalent cation-sensitive fluorophore COOH-FF6$(COOEt)_4$ to zymosan by carbodiimide-mediated activation (see Materials and Methods). The spectral properties of the covalent adduct are illustrated in Fig. 2. When emission is measured at 510 nm in medium devoid of divalent cations (pH 7.4), zymosan–FF6 displays an (uncorrected) excitation maximum at ~370 nm (Fig. 2 A). Addition of Ca^{2+} induces a blue shift in the excitation spectrum. The Ca^{2+}-saturated form of zymosan–FF6 has an excitation maximum at ~340 nm and the spectra display an isosbestic point near 360 nm (Fig. 2 A). Fluorescence intensity is modestly affected by pH, with only an ~10% drop at pH 4.5 (Fig. 2 B), the lower limit reported for phagosomal pH (40). By contrast, the fluorescence of zymosan–FF6 was effectively quenched by Mn^{2+} and, importantly, sensitivity to the metal persisted at pH 4.5 (Fig. 2 B). The probe was also effectively quenched by Fe^{2+} (Fig. 2 C) and Cu^{2+} (Fig. 2 D), whereas Zn^{2+} induced a modest fluorescence enhancement (Fig. 2 E). Therefore, zymosan–FF6 can be used to monitor the free concentration of divalent cations under the conditions prevailing in the phagosome. In the physiological concentra-

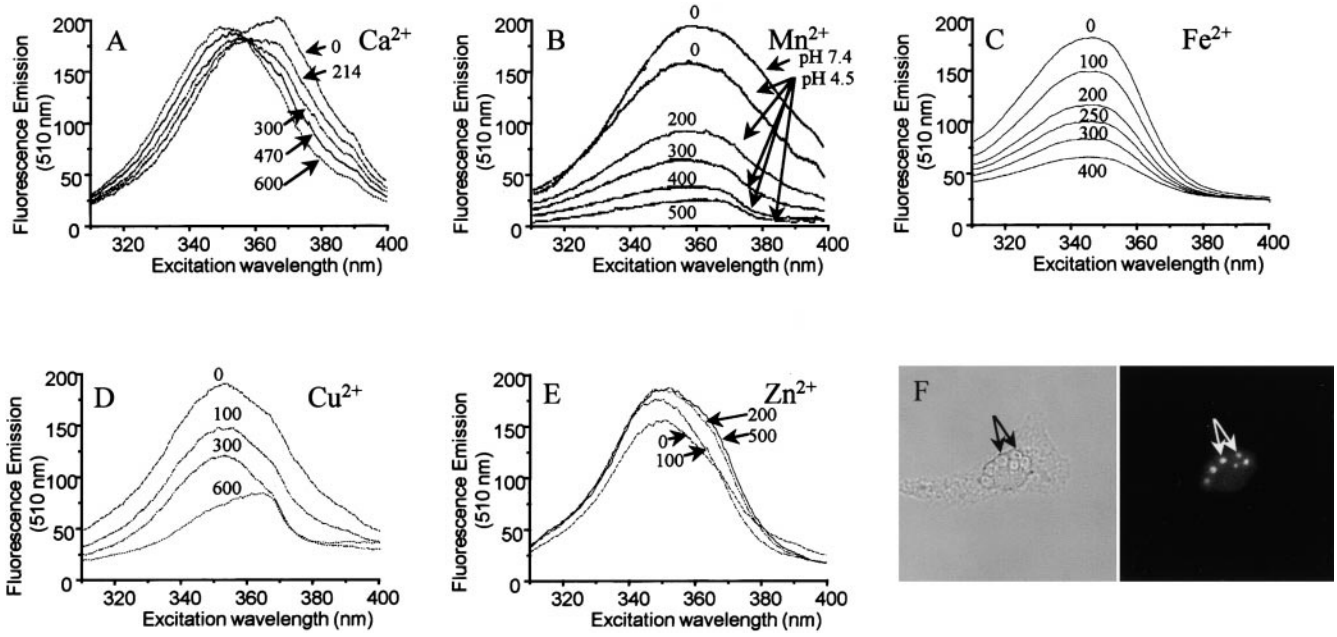

Figure 2. (A–E) Spectral properties of zymosan–FF6 particles in suspension. (A) Zymosan–FF6 particles were added to medium containing 140 mM KCl, 20 mM Hepes-Na (pH 7.4), and 500 μM EGTA, and the excitation spectrum was acquired with emission at 510 nm. Increasing amounts of Ca^{2+} were then added (total concentrations indicated) and fluorescence was recorded as above. (B–E) Zymosan–FF6 particles were added to medium containing 500 μM EGTA and 500 μM Ca^{2+} buffered at pH 7.4 or 4.5, as indicated, and excitation spectra were acquired (emission = 510 nm). Increasing amounts of Mn^{2+} (B), Fe^{2+} (C), Cu^{2+} (D), or Zn^{2+} (E) were then added (total concentrations indicated) and the effects of the divalent cations on zymosan–FF6 fluorescence were recorded. (F) Fluorescence properties of zymosan–FF6 particles ingested by macrophages. Peritoneal macrophages plated on coverslips were bathed in Ca^{2+}-free medium and allowed to ingest zymosan–FF6 particles for 30 min at 37°C. Coverslips were mounted in thermoregulated chambers and examined using differential interference contrast optics (left) and epifluorescence with excitation at 360 nm and emission at 535 nm (right). The location of zymosan–FF6 particles is indicated by arrows.

tion range, neither K^+ nor Mg^{2+} affected zymosan–FF6 fluorescence (not shown).

The zymosan–FF6 particles were effectively internalized by murine macrophages and could be readily visualized by differential interference contrast microscopy (Fig. 2 F, left). The fluorescence signal of internalized particles is bright with very low cellular background, and could be recorded by imaging using a cooled charge-coupled device camera (Fig. 2 F, right). Under the illumination conditions used, the fluorochrome of zymosan–FF6 underwent little photobleaching, with ≤1% loss of emission per exposure (not shown). Jointly, these features make zymosan–FF6 an appropriate probe to monitor cation fluxes in the phagosome.

Localization of Nramp1 at the Membrane of Zymosan-containing Phagosomes. In primary macrophages, Nramp1 is rapidly recruited to the membrane of phagosomes containing either latex beads (16) or live bacteria (18). To ensure that Nramp1 would also be recruited to the membrane of zymosan-containing phagosomes, peritoneal macrophages from normal (+/+) and *Nramp1* mutant (−/−) mice were allowed to ingest zymosan particles for 1 h at 37°C.

The cells were then fixed and analyzed for subcellular distribution of Nramp1 using an affinity-purified polyclonal antibody (13). Individual fields were analyzed under phase–contrast (Fig. 3, A and C) and examined for Nramp1 immunofluorescence (Fig. 3, B and D). In +/+ macrophages, ring-like Nramp1 staining was detected surrounding the internalized zymosan particle (Fig. 3 B). This staining was specific, as under otherwise identical conditions it was absent from phagosomes of macrophages isolated from −/− mice (Fig. 3 D). These results confirm that Nramp1 is recruited to the membrane of zymosan phagosomes.

Experimental Strategy. Having defined the location and sensitivity of the probe, as well as the differential presence of Nramp1 in zymosan-containing phagosomes of +/+ and −/− mice, we devised a strategy to quantify the rate of metal transport across the phagosomal membrane. For this purpose, we used Mn^{2+}, which was shown to effectively quench zymosan–FF6 fluorescence in vitro (Fig. 2 A). Mn^{2+} was chosen because, unlike the other cations tested, it is not subject to changes in redox state and is effectively transported by plasmalemmal divalent cation channels (see below). To minimize the contribution of Ca^{2+} to these measurements, we excited the probe at 360 nm, which was found to be near the isosbestic point for this cation (Fig. 2 A).

The phagosomal membrane is separated from the external milieu by the plasmalemma. To measure the permeability of the phagosomal membrane to Mn^{2+}, we therefore needed to ensure that the plasma membrane would not limit the access of the cation to the phagosome. To this end, the permeability of the plasma membrane to Mn^{2+} was greatly elevated by activation of its endogenous store-operated channels. This was accomplished by the depletion of Ca^{2+} stored in the endoplasmic reticulum with the sarco endoplasmic reticulum calcium ATPase inhibitor thapsigargin (41). As illustrated in Fig. 4, Mn^{2+} enters the cytosol of thapsigargin-treated cells rapidly, as measured using Fura-2 as a soluble cytosolic marker. Importantly, the rate of Mn^{2+} influx is similar in Nramp1-expressing and knockout macrophages. Elevation of the plasmalemmal permeability to divalent cations was used hereafter to gain access to the phagosomal membrane.

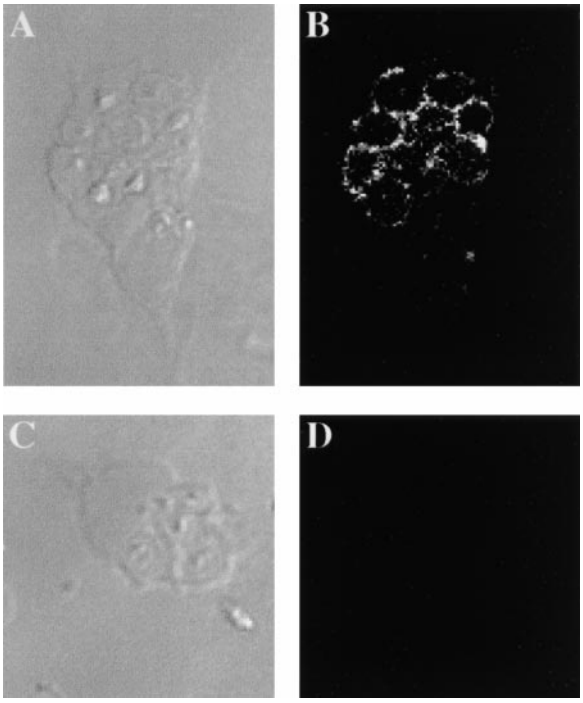

Figure 3. Nramp1 association with zymosan–FF6-containing phagosomes. Macrophages from normal mice (129sv, +/+; A and B) and from mutant mice with a null mutation at *Nramp1* (*Nramp1*$^{-/-}$, −/−; C and D) were harvested and plated on glass coverslips. After 48 h, the cells were allowed to ingest zymosan–FF6 for 1 h at 37°C. The cells were washed free of uningested particles and fixed before indirect immunofluorescence with an affinity-purified rabbit anti-Nramp1 antibody. Phase–contrast images (A and C) and the corresponding immunofluorescence micrographs (B and D) are shown.

Nramp1 Modulates the Phagosomal Mn^{2+} Content. The permeability of the phagosomal membrane to Mn^{2+} was studied next. Macrophages were allowed to internalize zymosan–FF6 in medium devoid of divalent cations to preclude fluorescence quenching during this period. Possible destruction of the dye by reactive oxygen species generated by the phagocyte was averted by inclusion of diphenylene iodonium, an inhibitor of the NADPH oxidase. A typical experiment is illustrated in Fig. 5 A. Thapsigargin was initially added to increase plasmalemmal permeability. In the absence of extracellular divalent cations this procedure had little effect on zymosan–FF6 fluorescence. However, subsequent addition of Mn^{2+} induced a rapid and sizable quenching of the fluorescent probe. This approach was used to compare the accumulation of Mn^{2+} in phagosomes from Nramp1 +/+ and −/− macrophages. The results of 17 individual experiments for +/+ macrophages and 15 experiments for −/− macrophages are summarized in Fig. 5 B. Importantly, fluorescence quenching was significantly higher in −/− macrophages compared with +/+ mac-

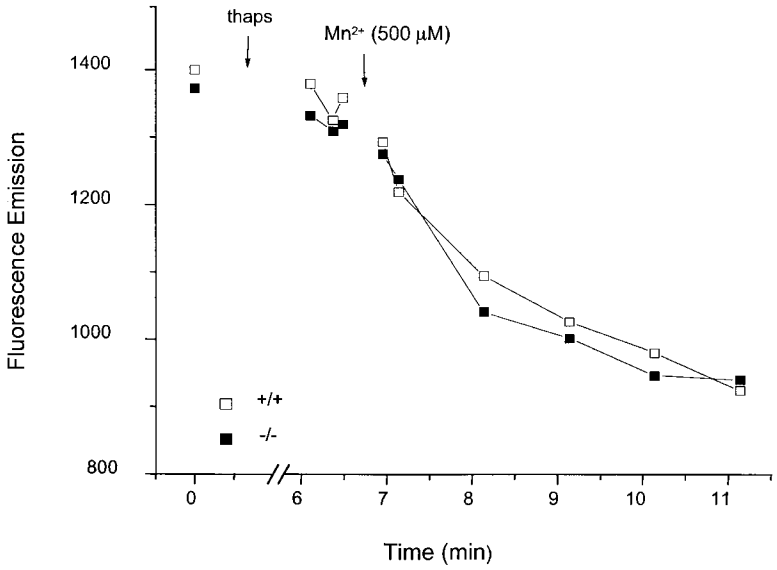

Figure 4. Quenching of cytosolic Fura-2 by Mn^{2+} in normal (+/+) and mutant (−/−) macrophages after treatment with thapsigargin. Peritoneal macrophages from normal (+/+) and *Nramp1* mutant (−/−) mice were plated on coverslips and loaded with Fura-2 by incubation with the precursor acetoxymethyl ester for 30 min at 37°C. Coverslips were mounted in thermoregulated chambers, the cells were bathed in Ca^{2+}-free medium containing 250 μM EGTA, and fluorescence was visualized with excitation at 360 nm. After recording baseline fluorescence, thapsigargin (thaps; 100 nM) was added to deplete calcium stores and open store–operated channels. Finally, 500 μM Mn^{2+} was added and recording was resumed. Data are representative of three similar experiments.

rophages, and, using a time-series analysis, the difference was highly significant at all time points ($P < 0.001$). In addition, comparing quenching between 3 and 6 min in both groups suggests a significantly faster rate of quenching in −/− than +/+ macrophages. Quenching was optimal at 7 min (−/−, 56 ± 4%; +/+, 22 ± 1%), and there was no additional reduction in signal intensity in either cell types upon prolonged measurements up to 12 min.

The rate of quenching of zymosan–FF6 is an indication of the net changes in phagosomal Mn^{2+} content over time. Because the phagosomal Mn^{2+} content is dictated by the rates of influx and efflux of the metal, the faster rate of quenching observed in −/− cells could result from elevated influx (from cytosol to lumen) or from decreased efflux (from lumen to cytosol). To discern between these possibilities, we estimated the unilateral rate of efflux by preloading zymosan–FF6 phagosomes with Mn^{2+} during the course of phagocytosis. This was accomplished by incubating zymosan–FF6 particles with 1 M Mn^{2+} for 30 min at room temperature before feeding them to macrophages. Under these conditions, the fluorescence is largely quenched at the onset of phagocytosis. The reappearance of fluorescence when the cells are bathed in a medium devoid of divalent metals provides an estimate of the rate of Mn^{2+} efflux. After 30 min, at which time Nramp1 is known to be recruited to the phagosomal membrane, the mean fluorescence intensity was greater in phagosomes from +/+ macrophages than in their −/− counterparts. In 121 phagosomes from +/+ mice, the fluorescence intensity averaged 590 ± 8 units, whereas in 95 phagosomes from −/− animals the fluorescence was 363 ± 10 units (means ± SE). These values are significantly different ($P < 0.0001$). The greater fluorescence recorded in Nramp1-expressing macrophages is indicative of a greater ability to extrude Mn^{2+} from the lumen of their phagosomes.

To more precisely define the onset of the Mn^{2+} efflux period, cells were allowed to form phagosomes in media containing both Mn^{2+} (200 μM) and TPEN (400 μM), a

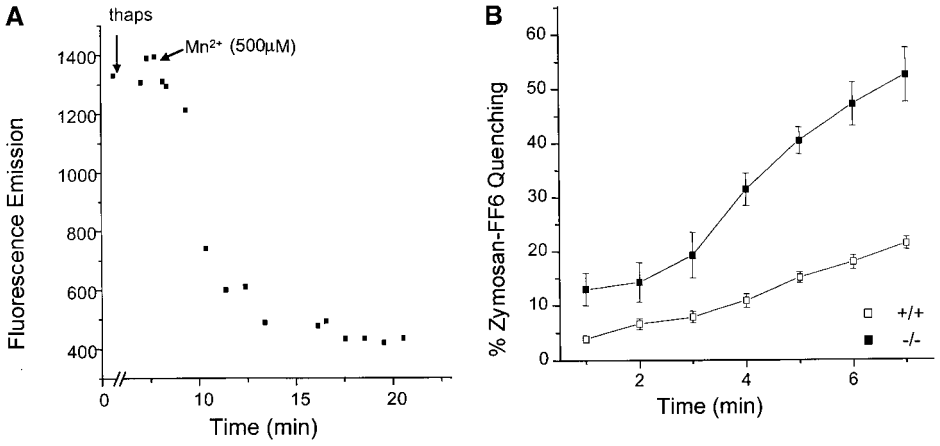

Figure 5. The effect of Nramp1 expression on Mn^{2+}-induced quenching of internalized zymosan–FF6 fluorescence. Peritoneal macrophages from normal (+/+) and *Nramp1* mutant (−/−) mice were plated for 48 h on coverslips, and allowed to ingest zymosan–FF6 particles for 30 min at 37°C in Ca^{2+}-free medium containing 250 μM EGTA. Coverslips were mounted in thermoregulated chambers and examined using differential interference contrast optics to locate internalized particles. Fluorescence was measured with excitation at 360 nm before and after addition of 100 nM thapsigargin (thaps). Mn^{2+} (500 μM) was added to the cells where indicated and recording was resumed. A illustrates a typical experiment, and B summarizes the fractional quenching (as percentage of initial fluorescence) as a function of time. Data in B are means ± SE of 15 individual experiments for −/− macrophages (filled symbols) and 17 experiments for +/+ macrophages (open symbols).

divalent cation chelator with high affinity towards Mn^{2+} ($K_d = 5.4 \times 10^{-11}$). The presence of TPEN served to stabilize the concentration of the metal throughout the stages of phagosome formation and maturation. In addition, because the chelator is membrane permeant (42, 43), sudden removal of TPEN from the solution imposes an outward gradient and promotes its rapid loss from the phagosomes. As divalent cations are comparatively much less permeant, the net loss of TPEN results in the sudden appearance of free Mn^{2+} within the phagosomal lumen, which in turn binds to and quenches zymosan–FF6. It is then possible to monitor the reappearance of fluorescence as a measure of Mn^{2+} efflux. 10 min after removal of the chelator, the fluorescence of +/+ phagosomes averaged 51 ± 3% ($n = 5$), whereas in −/−cells it was only 21.5 ± 3% ($n = 5$; $P < 0.0001$). In view of these findings, the differential rate of quenching noted in the experiments of Fig. 5 can be most simply explained by more effective extrusion of incoming Mn^{2+} from Nramp1-expressing phagosomes. These findings are consistent with the ability of Nramp1 to translocate divalent metals from the lumen of the phagosome to the cytosol.

Transport of Manganese by Nramp1 Is pH Dependent. Studies in *Xenopus laevis* oocytes (21) and Caco-2 cells (44) indicate that divalent cation transport by Nramp2 is pH dependent, activated by acidity. Indeed, it has been suggested that H^+ (equivalents) are cotransported with the divalent cation through an rheogenic symporter (45). As Nramp1 is structurally similar to Nramp2 and is expressed in organelles known to have an acidic lumen, it is conceivable that it is similarly pH dependent. The possible pH dependence of Nramp1 was investigated by comparing the rate of Mn^{2+} accumulation in the presence and absence of a TM pH gradient. Acidification of the phagosome is dependent on recruitment and activity of the vacuolar H^+-ATPase (44), which is exquisitely sensitive to inhibition by macrolide antibiotics like concanamycin and bafilomycin (46). Therefore, these compounds were used to obliterate the phagosomal acidification. Their effectiveness was initially verified using opsonized particles that were covalently derivatized with two pH-sensitive fluorescent dyes with different pK_a values, to extend the dynamic range of the measurements. As shown in Fig. 6 A, the resting phagosomal pH of −/− and +/+ macrophages is indistinguishable, averaging 4.5 in three individual experiments. Addition of concanamycin induced rapid and complete dissipation of the TM ΔpH in both cases (Fig. 6 A). It is noteworthy that thapsigargin, the agent used to elevate plasmalemmal cation permeability, had no detectable effect on phagosomal H^+ (equivalent) permeability.

Having defined the time required to dissipate the pH gradient, we proceeded to test the effects of concanamycin on Mn^{2+} accumulation. After addition of concanamycin and permeabilization of the surface membrane with thapsigargin, addition of Mn^{2+} promoted a rapid quenching of zymosan–FF6 (Fig. 6 B). Importantly, the rate of quenching in +/+ macrophages was faster than observed in the absence of the V-ATPase inhibitor (Figs. 5 B and 6 B). As a result, the difference in the rate of net Mn^{2+} uptake between +/+ and −/− cells was not statistically significant after 3 min (2 min, $P < 0.05$; 3 min, $P > 0.01$) and became negligible after 4 min (Fig. 6 B). These findings imply that, as in the case of Nramp2, metal translocation by Nramp1 is pH dependent and dissipation of the phagosomal acidification reduces transport to negligible levels so that the contribution of Nramp1 becomes undetectable.

Discussion

Although genetic analyses in mice and humans have established the key role of *Nramp1* in resistance to intracellular infections and macrophage antimicrobial functions, the

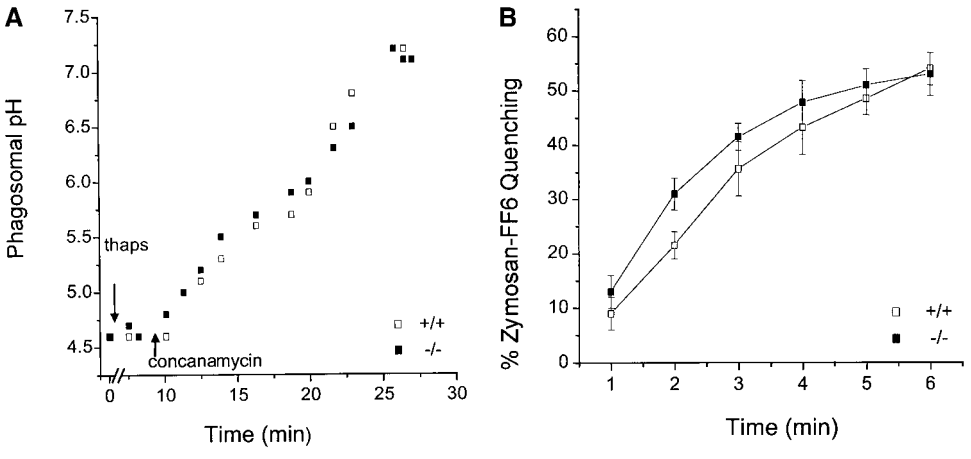

Figure 6. Effect of pH on Mn^{2+} transport across the phagosomal membrane. (A) Phagosomal pH was measured by ratio imaging in peritoneal macrophages from normal (+/+; open symbols) and *Nramp1* mutant (−/−; filled symbols) mice, using zymosan covalently conjugated to FITC and Oregon green 514, as described in Materials and Methods. Fluorescence at 535 nm was measured with alternating excitation at 440 and 490 nm. Where indicated, the cells were treated with 100 nM thapsigargin (thaps), followed by 100 nM concanamycin. For calibration, the cells were permeabilized with 1% Triton X-100 and sequentially perfused with solutions at pH 7.5, 7, 6.5, 5.5, 4.5, and 4. Results are representative of three determinations for each type of macrophage. (B) Effect of the vacuolar H^+-ATPase inhibitor concanamycin on the Mn^{2+}-induced quenching of fluorescence of phagosomal zymosan–FF6 in normal (+/+; open symbols) and *Nramp1* mutant (−/−; filled symbols) macrophages. The experiment was carried out as described in the legend to Fig. 5 B, except that the cells were pretreated with 100 nM of concanamycin for 25 min to allow inhibition dissipation of the phagosomal acidification, before the addition of thapsigargin and finally Mn^{2+}. The data are means ± SE of eight individual experiments.

molecular basis of Nramp1 action at the phagosomal membrane has remained difficult to elucidate. A role as a transporter has been postulated, but the possible transport substrate, the direction of transport, and how this transport activity affects microbial survival and/or replication remain unknown.

Divalent metals such as Fe^{2+}, Mn^{2+}, and Zn^{2+} are known to play an important role in host defense against infections (for a review, see reference 47), by acting as important cofactors for the production of toxic hydroxyl radicals or for bacterially encoded detoxifying metalloenzymes such as superoxide dismutase (48–50). These functions in innate immunity make divalent metals attractive substrates for Nramp1. In addition, macrophages are also essential for the recycling of iron from the breakdown of effete red cells (51, 52). This prompted the suggestion that Nramp1 may function as a macrophage-specific iron transporter at the phagosomal membrane (53). However, to date the analysis of Nramp1 function has been hampered by its restricted targeting to the lysosomal compartment of primary macrophages and transfected cells (16, 24). The absence of the protein from the plasma membrane has precluded functional studies in intact cells using isotopic cations or fluid-phase fluorescent markers. Indeed, unlike Nramp2, transfection and overexpression of Nramp1 in Chinese hamster ovary and other cell types does not cause increased pH-dependent $^{55}Fe^{2+}$ uptake (Picard, V., and P. Gros, unpublished data). Likewise, although Nramp2 expression can functionally complement a double *smf1/smf2* yeast mutant, Nramp1 fails to do so (31). Nevertheless, several published reports have attempted to link Nramp1 to Fe^{2+} transport in macrophages, though the results have been contradictory. In one study (36), it was observed that increased Fe^{2+} levels enhance *Mycobacterium avium* replication in Bcg^r mice, while in another (37), an inhibitory effect was observed. Atkinson and Barton recently reported reduced $^{55}Fe^{2+}$ uptake in Nramp1-transfected RAW macrophages compared with control RAW cells, but observed the opposite effect when quenching of calcein was used to monitor intracellular Fe^{2+} (54). These authors concluded that Nramp1 may transport Fe^{2+} out of the phagosome but out of the cells as well, via an endocytic pathway (54). Independently, Zwilling et al. (36) and Khun et al. (55) reported that isolated phagosomes from *Nramp1*-transfected cells accumulate more iron ($^{55}Fe^{2+}$) than controls, suggesting that Nramp1 transports Fe^{2+} into the phagosome. They further postulated that intraphagosomal Fe^{2+} would serve as a catalyst in the Haber-Weiss reaction, generating highly toxic hydroxyl radicals in the microenvironment surrounding the pathogen. This model appears unlikely, as the direction of transport catalyzed by Nramp1 would have to be opposite to that of Nramp2 with respect to membrane polarity and, most importantly, with respect to the pH gradient. These seemingly conflicting results highlight the need for more systematic approaches to study Nramp1 transport

The goal of this study was to devise a divalent cation-sensitive fluorescent probe that could be incorporated in the phagosome, where it could be used to monitor the effect of Nramp1 recruitment on divalent cation transport in intact cells. Zymosan particles conjugated to Fura-FF6 (zymosan–FF6) proved ideal for this study for the following reasons: (a) zymosan particles are avidly ingested by mature macrophages without the need for opsonization, and are fairly large (2–4 μm), facilitating detection after phagocytosis; (b) zymosan particles are porous and thus generate phagosomes with a significant aqueous space where ion fluxes can be monitored (as opposed to solid latex beads); (c) when measured at the isosbestic wavelength (~360 nm), Fura-FF6 fluorescence is Ca^{2+} insensitive, which eliminates any contribution of this cation to the measurements; and (d) Fura-FF6 fluorescence is fairly resistant to photobleaching and relatively insensitive to pH, which allows repeated image acquisition in the acidified environment of the mature phagosome.

In this study, microfluorescence imaging of zymosan–FF6 particles internalized by wild-type 129sv and by syngeneic Nramp1$^{-/-}$ primary macrophages was used to monitor the effect of Nramp1 on Mn^{2+} content of the phagosome in intact live cells, in real time and under near physiological conditions. Although Mn^{2+} was used for technical reasons (see above), it is important that our results do not imply that this is the sole or even the most important cation transported by Nramp1. Collectively, our observations indicate that Nramp1 functions as a pH-dependent transporter that can extrude divalent metals (Mn^{2+}) from the intraphagosomal space. This conclusion contrasts with that of Zwilling et al. (36) and Khun et al. (55), who suggested that Nramp1 could transport divalent metals into the phagosome. The reason for the discrepancy between their results and ours is unclear, but may be linked to the different experimental systems and conditions used. Nramp1 may be capable of transport in both directions, in which case the net flux will be dictated by the combined electrochemical gradients of the metal and H^+. Under our conditions, which detect net changes in the content, the predominant flux would be outward (lumen to cytosol). Nevertheless, when measured isotopically, metal uptake could be detected in either direction. Because of the tendency of divalent metals to bind to biological surfaces, we feel that the zymosan–FF6 and related methods are preferable to isotopic determinations.

The Nramp1 activity measured here is in agreement with its structural similarity to Nramp2 and other Nramp homologues, and with the known functional characteristics of these homologues. First, Nramp1 and Nramp2 can both transport divalent cations, such as Mn^{2+} (this study and reference 21). Second, both Nramp1 and 2 are sensitive to the pH on the same (cis) side where the metal is transported from. The two proteins are predicted to have nearly identical secondary structure and therefore also identical TM disposition. Because Nramp2 translocates metals into the cell, the organellar localization of Nramp1 predicts that it will transport metals from the vesicular lumen, the topological equivalent of the extracellular space, into the cytosol. The predicted direction of transport is in agreement with our observations. Finally, thermodynamic considerations also

support the notion that net transport occurs outwardly. The phagosomal lumen is acidified to pH 4.5–5.5 by active V-ATPases. These ATPases are electrogenic, raising the possibility that the phagosomal lumen is, in addition, electropositive. The combined electrochemical gradient would be poised to effectively extrude metals from the phagosome. Accordingly, we find that Mn^{2+} extrusion via Nramp1 is obliterated by pretreatment of the cells with concanamycin, a specific V-ATPase inhibitor.

It is noteworthy that Mn^{2+} readily enters phagosomes in Nramp1-deficient macrophages. This implies that other transporters for the metal exist in these membranes. In fact, in addition to Nramp proteins, two other high affinity transport systems for divalent cations have been described, the heavy metal (CPx-type) ATPase and members of the family of facilitated diffusion transporters (for a review, see reference 56). In addition, Mn^{2+} can traverse divalent cation-specific and nonselective cation channels (56, 57). In the absence of a gradient that preferentially favors transport via Nramp1, these systems could obscure the contribution of the latter. This condition may have prevailed in some of the studies using isolated phagosomes, in which the protonmotive gradient would have been altered.

What are the expected consequences of divalent metal depletion from the phagosomal space on the antimicrobial defense system of phagocytes? Intracellular pathogens such as *Salmonella typhimurium*, *M. tuberculosis*, *Mycobacterium bovis*, and *Leishmania donovani* synthesize superoxide dismutase (58–60), an important component of the intracellular survival strategy of these pathogens. Importantly, Mn^{2+} is an essential cofactor for superoxide dismutase and elimination of the cation from the phagosomal milieu would result in inactivation of this protective enzymatic activity, resulting in a net enhancement of the bactericidal activity of the phagocyte. Such a mechanism would provide an attractive explanation for the observed pleiotropic effect of *Nramp1* mutations on the susceptibility to infection with phylogenetically unrelated intracellular pathogens such as *Salmonella*, *Mycobacteria*, and *Leishmania* (1–3). Nramp1 may also transport, in addition to Mn^{2+} ions, other divalent cations such as Fe^{2+} or Zn^{2+}, which together may be essential to the general metabolic activity of intracellular parasites, including expression of virulence determinants responsible for inhibition of phagolysosome fusion noted for some of these pathogens (20). Indeed, *Mycobacteria* are known to survive intracellularly by prematurely arresting the process of phagosome maturation (reduced acidification, reduced fusion to lysosomes, and retention of endosomal markers [61, 62]). We have observed in primary macrophages (129sv, *Nramp1*$^{-/-}$) and in Nramp1-cMyc–transfected RAW macrophages that in the presence of a functional Nramp1, mycobacterial phagosomes acidify more fully (pH 5.5), whereas their counterparts in macrophages lacking Nramp1 remain immature and acidify only partially (pH 6.5 [18, 19]). This Nramp1 effect is specific to mycobacterial phagosomes and was not seen in phagosomes containing either dead bacilli or inert latex beads, which both acidify fully to pH 5.5 in the presence or absence of Nramp1. This difference in pH was due to a reduced bafilomycin-sensitive activity of V-ATPase, associated with reduced recruitment of V-ATPase and of the lysosomal marker Lamp-2 (19). In addition, comparative electron microscopy studies of *M. avium* phagosomes formed in wild-type and *Nramp1* mutant macrophages show that increased microbial replication in *Nramp1* mutant macrophages is associated with reduction of phagosome fusion to BSA-Au–labeled lysosomes (20). Thus, the mycobacterial capacity to inhibit phagolysosome fusion is reduced in the presence of a functional host Nramp1 protein in the phagosomal membrane.

Microbial genome sequencing projects have recently identified Nramp homologues in many bacterial species, including *Salmonella* and *Mycobacteria*, which share 25–30% sequence identity between themselves and their mammalian counterparts (34, 35). The *M. tuberculosis* Mramp homologue was recently studied in *Xenopus* oocytes and shown to be capable of transporting Fe^{21} (34). Likewise the *MntH* homologue from *E. coli* was functionally characterized (35). Overexpression of the MntH protein can rescue the metal-sensitive phenotype of a temperature-sensitive *E. coli* mutant, hflB1(Ts), and direct transport measurements showed that it can mediate a CCCP-sensitive, pH-dependent uptake of both Fe^{2+} and Mn^{2+} in intact cells. These findings suggest that both the macrophage Nramp1 and the microbial Nramp homologues may function in opposite direction, likely competing for Mn^{2+} and/or other metals in the microenvironment of the phagosome.

In summary, we provided evidence that Nramp1 functions as an H^+-sensitive divalent cation transporter in the membrane of intact phagosomes in situ. Because of their ability to transport metals and because they are expressed by both phagocytes and pathogens, members of the Nramp superfamily of proteins appear to play a key role at the host–parasite interface in the microenvironment of the phagosome.

This work was supported by National Institutes of Health grant 1R01 A135237-06 to P. Gros, and Medical Research Council of Canada and National Sanatorium Association grants to S. Grinstein. N. Jabado is the recipient of a Human Science Frontier fellowship. P. Gros and S. Grinstein are International Scholars of the Howard Hughes Medical Institute and Career Scientists of the Medical Research Council of Canada. S. Grinstein is the current holder of the Pitblado Chair in Cell Biology.

Submitted: 9 June 2000
Revised: 21 August 2000
Accepted: 15 September 2000

References

1. Skamene, E., E. Schurr, and P. Gros. 1998. Infection genomics: Nramp1 as a major determinant of natural resistance to intracellular infections. *Annu. Rev. Med.* 49:275–285.
2. Govoni G., and P. Gros. 1998. Macrophage NRAMP1 and its role in resistance to microbial infections. *Inflamm. Res.* 47: 277–284.
3. Vidal, S.M., D. Malo, K. Vogan, E. Skamene, and P. Gros. 1993. Natural resistance to infection with intracellular para-

sites: isolation of a candidate for Bcg. *Cell.* 73:469–485.
4. Malo, D., K. Vogan, S. Vidal, J. Hu, M. Cellier, E. Schurr, A. Fuks, N. Bumstead, K. Morgan, and P. Gros. 1994. Haplotype mapping and sequence analysis of the mouse Nramp gene predict susceptibility to infection with intracellular parasites. *Genomics.* 23:51–61.
5. Vidal, S., M.L. Tremblay, G. Govoni, S. Gauthier, G. Sebastiani, D. Malo, E. Skamene, M. Olivier, S. Jothy, and P. Gros. 1995. The Ity/Lsh/Bcg locus: natural resistance to infection with intracellular parasites is abrogated by disruption of the *Nramp1* gene. *J. Exp. Med.* 182:655–666.
6. Bellamy, R., C. Ruwende, T. Corrah, K.P. McAdam, H.C. Whittle, and A.V. Hill. 1998. Variations in the NRAMP1 gene and susceptibility to tuberculosis in West Africans. *N. Engl. J. Med.* 338:640–644.
7. Bellamy, R. 2000. Identifying genetic susceptibility factors for tuberculosis in Africans: a combined approach using a candidate gene study and a genome-wide screen. *Clin. Sci.* 98:245–250.
8. Abel, L., F.O. Sanchez, J. Oberti, N.V. Thuc, L.V. Hoa, V.D. Lap, E. Skamene, P.H. Lagrange, and E. Schurr. 1998. Susceptibility to leprosy is linked to the human NRAMP1 gene. *J. Infect. Dis.* 177:133–145.
9. Greenwood, C.M.T., T.M. Fujiwara, L.J. Boothroyd, M.A. Miller, D. Frappier, E.A. Fanning, E. Schurr, and K. Morgan. 2000. Linkage of tuberculosis to chromosome 2q35 loci, including *NRAMP1*, in a large aboriginal Canadian family. *Am. J. Hum. Genet.* 67:405–416.
10. Shaw, M.A., A. Collins, C.S. Peacock, E.N. Miller, G.F. Black, D. Sibthorpe, Z. Lins-Laison, J.J Shaw, F. Ramos, F. Silveira, and J.M. Blackwell. 1997. Evidence that genetic susceptibility to *Mycobacterium tuberculosis* in a Brazilian population is under oligogenic control: linkage study of the candidates genes *NRAMP1* and *TNF*A. *Tuber. Lung Dis.* 78: 35–45.
11. Govoni, G., S. Gauthier, F. Billia, N.N. Iscove, and P. Gros. 1997. Cell-specific and inducible Nramp1 gene expression in mouse macrophages in vitro and in vivo. *J. Leukoc. Biol.* 62: 277–286.
12. Cellier, M., C. Shustik, W. Dalton, E. Rich, J. Hu, D. Malo, E. Schurr, and P. Gros. 1997. Expression of the human NRAMP1 gene in professional primary phagocytes: studies in blood cells and in HL-60 promyelocytic leukemia. *J. Leukoc. Biol.* 61:96–105.
13. Vidal, S.M., E. Pinner, P. Lepage, S. Gauthier, and P. Gros. 1996. Natural resistance to intracellular infections: Nramp1 encodes a membrane phosphoglycoprotein absent in macrophages from susceptible (Nramp1 D169) mouse strains. *J. Immunol.* 157:3559–3568.
14. Cellier, M., G. Prive, A. Belouchi, T. Kwan, V. Rodrigues, W. Chia, and P. Gros. 1995. Nramp defines a family of membrane proteins. *Proc. Natl. Acad. Sci. USA.* 92:10089–10093.
15. Cellier, M., A. Belouchi, and P. Gros. 1996. The *Nramp* gene and resistance to intracellular infections: can genome comparative analysis help understand its function? *Trends Genet.* 12: 201–204.
16. Gruenheid, S., E. Pinner, M. Desjardins, and P. Gros. 1997. Natural resistance to infection with intracellular pathogens: the Nramp1 protein is recruited to the membrane of the phagosome. *J. Exp. Med.* 185:717–730.
17. Blackwell, J.M. 1996. Structure and function of the natural resistance associated macrophage protein (Nramp1), a candidate for infectious and auto-immune disease susceptibility. *Mol. Med. Today.* 1:205–211.
18. Govoni, G., F. Cannone-Hergaux, C.G. Pfeifer, S. Marcus, S. Mills, D. Hackam, S. Grinstein, D. Malo, B. Finlay, and P. Gros. 1999. Functional expression of Nramp1 *in vitro* after transfection into the murine macrophage line RAW264.7. *Infect. Immun.* 67:2225–2232.
19. Hackam, D.J., O.D. Rotstein, W. Zhang, S. Gruenheid, P. Gros, and S. Grinstein. 1998. Host resistance to intracellular infection: mutation of natural resistance–associated macrophage protein 1 (Nramp1) impairs phagosomal acidification. *J. Exp. Med.* 188:351–364.
20. de Chastellier, C., and L. Thilo. 1997. Phagosome maturation and fusion with lysosomes in relation to surface property and size of the phagocytic particle. *Eur. J. Cell Biol.* 74:49–62.
21. Gunshin, H., B. Mackenzie, U.V. Berger, Y. Gunshin, M.F. Romero, W.F. Boron, S. Nussberger, J.L. Gollan, and M.A. Hediger. 1997. Cloning and characterization of a mammalian proton-coupled metal-ion transporter. *Nature.* 388:482–488.
22. Flemming, R.E., M.C. Migas, X. Zhou, J. Jiang, R.S. Britton, E.M. Brunt, S. Tomatsu, A. Waheed, B.R. Bacon, and W.S. Sly. 1999. Mechanism of increased iron absorption in murine model of hereditary hemochromatosis: increased duodenal expression of the iron transporter DMT1. *Proc. Natl. Acad. Sci. USA.* 96:3143–3148.
23. Gruenheid, S., M. Cellier, S. Vidal, and P. Gros. 1995. Identification and characterization of a second mouse Nramp gene. *Genomics.* 25:514–525.
24. Gruenheid, S., F. Cannone-Hergaux, S. Gauthier, D.J. Hackam, S. Grinstein, and P. Gros. 1999. The iron transport protein Nramp2 is an integral membrane protein that colocalizes with transferrin in recycling endosomes. *J. Exp. Med.* 189:831–841.
25. Tabuchi, M., T. Yoshimori, K. Yamagushi, T. Yoshida, and F. Kishi. 2000. Human NRAMP2/DMT1, which mediates iron transport across endosomal membranes, is localized to late endosomes and lysosomes in HEp-2 cells. *J. Biol. Chem.* 275:22220–22228.
26. Cannone-Hergaux, F., S. Gruenheid, P. Ponka, and P. Gros. 1999. Cellular and subcellular localization of the Nramp2 iron transporter in the intestinal brush border and regulation by iron. *Blood.* 93:4406–4417.
27. Fleming, M.D., C.C. Trenor III, M.A. Su, D. Foernzler, D.R. Beier, W.F. Dietrich, and N.C. Andrews. 1997. Microcytic anaemia mice have a mutation in Nramp2, a candidate iron transporter gene. *Nat. Genet.* 16:383–386.
28. Fleming, M.D., M.A. Romano, M.A. Su, L.M. Garrick, M.D. Garrick, and N.C. Andrews. 1998. Nramp2 is mutated in the anemic Belgrade (b) rat: evidence of a role for Nramp2 in endosomal iron transport. *Proc. Natl. Acad. Sci. USA.* 95: 1148–1153.
29. Supek, F., L. Supekova, H. Nelson, and N. Nelson. 1996. A yeast manganese transporter related to the macrophage protein involved in conferring resistance to mycobacteria. *Proc. Natl. Acad. Sci. USA.* 93:5105–5110.
30. Liu, X.F., and V.C. Culotta. 1999. Post-translational control of Nramp metal transport in yeast. *J. Biol. Chem.* 274:4863–4868.
31. Pinner, E., S. Gruenheid, M. Raymond, and P. Gros. 1997. Functional complementation of the yeast divalent cation transporter family SMF by NRAMP2, a member of the mammalian natural resistance-associated macrophage protein

family. *J. Biol. Chem.* 272:28933–28938.
32. Orgad, S., H. Nelson, D. Segal, and N. Nelson. 1998. Metal ions suppress the abnormal taste behavior of the *Drosophila* mutant *malvolio*. *J. Exp. Biol.* 201:115–120.
33. D'Sousa, J., P.W. Cheah, P. Gros, W. Chia, and V. Rodrigues. 1999. Functional complementation of the *malvolio* mutation in the taste pathway of *Drosophila* by the human natural resistance-associated macrophage protein 1 (NRAMP-1). *J. Exp. Biol.* 202:1909–1915.
34. Agranoff, D., I.M. Monahan, J.A. Mangan, P.D. Butcher, and S. Krishna. 1999. *Mycobacterium tuberculosis* expresses a novel pH-dependent divalent cation transporter belonging to the Nramp family. *J. Exp. Med.* 190:717–724.
35. Makui, H., E. Roig, S.T. Cole, J.D. Helmann, P. Gros, and M. Cellier. 2000. Identification of *Escherichia coli* K-12 Nramp (MntH) as a selective divalent metal ion transporter. *Mol. Microbiol.* 35:1065–1078.
36. Zwilling, B.S., D.E. Kuhn, L. Wikoff, D. Brown, and W. Lafuse. 1999. Role of iron in Nramp1-mediated inhibition of mycobacterial growth. *Infect. Immun.* 67:1386–1392.
37. Atkinson, P.G.P., and C.H. Barton. 1998. Ectopic expression of Nramp1 in COS-1 cells modulates iron accumulation. *FEBS Lett.* 425:239–242.
38. Gomes, M.S., and R. Appelberg. 1998. Evidence for a link between iron metabolism and Nramp1 gene mediated inhibition of mycobacterial growth. *Immunology.* 95:165–172.
39. Colette, J., D. McGreer, R. Crawford, F. Chubb, and R.D. Sandin. 1956. Synthesis of some cyclic iodonium salts. *J. Am. Chem. Soc.* 78:3819–3820.
40. Greenberg, S., and S.C. Siverstein. 1993. Phagocytosis. *In* Fundamental Immunology. W.E. Paul, editor. Raven Press, New York. 941–964.
41. Ma, H., L. Zhong, G. Inesi, I. Fortea, F. Soler, and F. Fernandez-Belda. 1999. Overlapping effects of S3 stalk segment mutations on the affinity of $Ca2^{+}$-ATPase (SERCA) for thapsigargin and cyclopiazonic acid. *Biochemistry.* 38: 15522–15527.
42. Baba, A., S. Etoh, and H. Iwata. 1991. Inhibition of NMDA-induced protein kinase C translocation by a Zn^{2+} chelator: implication of intracellular Zn^{2+}. *Brain Res.* 557:103–108.
43. Arslan, P., F. Di Virgilio, M. Beltrame, R.Y. Tsien, and T. Pozzan. 1985. Cytosolic Ca^{2+} homeostasis in Ehrlich and Yoshida carcinomas. A new, membrane-permeant chelator of heavy metals reveals that these ascites tumor cell lines have normal cytosolic free Ca^{2+}. *J. Biol. Chem.* 260:2719–2727.
44. Tandy, S., M. Williams, A. Leggett, M. Lopez-Jimenez, M. Dedes, B. Ramesh, S.K. Srai, and P. Sharp. 2000. Nramp2 expression is associated with pH-dependent iron uptake across the apical membrane of human intestinal Caco-2 cells. *J. Biol. Chem.* 275:1023–1029.
45. Luckas, G.L., O.D. Rotstein, and S. Grinstein. 1991. Determinants of the phagosomal pH in macrophages: *in situ* assessment of vacuolar H^{+}-ATPase activity, counterion conductance and H^{+} leak. *J. Biol. Chem.* 266:24540–24548.
46. Hackam, D.J., O.D. Rostein, W.J. Zhang, N. Demaurex, M. Woodside, O. Tsai, and S. Grinstein. 1997. Regulation of phagosomal acidification. Differential targeting of Na^{+}/H^{+} exchangers. Na^{+}/K^{+} ATP-ases, and vacuolar type H^{+}-ATP-ases. *J. Biol. Chem.* 272:29810–29820.
47. Kontoghioghes, G.J., and E.D. Weinberg. 1995. Iron: mammalian defense systems, mechanisms of disease and chelation therapy approaches. *Blood Rev.* 9:33–45.
48. Hampton, M.B., A.J. Kettle, and C.C. Winterbourn. 1998. Inside the neutrophil phagosome: oxydants, myeloperoxidase and bacterial killing. *Blood.* 92:3007–3017.
49. Crosa, J.H. 1997. Signal transduction and transcriptional and post-transcriptional control of iron-regulated genes in bacteria. *Microbiol. Mol. Biol. Rev.* 61:319–336.
50. Agranoff, D.A., and S. Krishna. 1999. Metal ion homeostasis and intracellular parasitism. *Mol. Microbiol.* 28:403–412.
51. Kondo, H., K. Saito, J.P. Grasso, and P. Aisen. 1988. Iron metabolism in the erythrophagocytosing Kupffer cell. *Hepatology.* 8:28–32.
52. Kay, M.M.B. 1975. Mechanism of removal of senescent cells by human macrophages *in situ*. *Proc. Natl. Acad. Sci. USA.* 72: 3521–3525.
53. Andrews, N.C., and J.E. Levy. 1998. Iron is hot: an update on the pathophysiology of hemochromatosis. *Blood.* 92: 1845–1851.
54. Atkinson, P.G.P., and C.H. Barton. 1999. High level expression of Nramp1G169 in RAW 1264.7 cell transfectants: analysis of intracellular iron transport. *Immunology.* 96:656–662.
55. Kuhn, D.E., B.D. Baker, W.P. Lafuse, and B.S. Zwilling. 1999. Differential iron transport into phagosomes isolated from the RAW264.7 macrophage cell lines transfected with Nramp1Gly169 or Nramp1Asp169. *J. Leukoc. Biol.* 66:113–119.
56. Williams, L.E., J.K. Pittman, and J.L. Hall. 2000. Emerging mechanisms for heavy metal transport in plants. *Biochim. Biophys. Acta.* 1465:104–126.
57. Kehres, D.G., M.L. Zaharik, B.B. Finlay, and M.E. Maguire. 2000. The NRAMP proteins of *Salmonella typhimurium* and *Escherichia coli* are selective manganese transporters involved in the response to reactive oxygen. *Mol. Microbiol.* 36:1085–1110.
58. Tsolis, R.M., A.J. Baumler, and F. Heffron. 1995. Role of *Salmonella typhimurium* Mn-superoxide dismutase (SodA) in protection against early killing by J774 macrophages. *Infect. Immun.* 63:1739–1744.
59. Zhang, Y., R. Lathigra, T. Garbe, D. Catty, and D. Young. 1991. Genetic analysis of superoxide dismutase, the 23 kilodalton antigen of *Mycobacterium tuberculosis*. *Mol. Microbiol.* 5:381–391.
60. Dey, R., and S.C. Datta. 1994. Leishmanial glycosomes contain superoxide dismutase. *Biochem. J.* 301:317–319.
61. Clemens, D.L., and M.A. Horwitz. 1995. Characterization of the *Mycobacterium tuberculosis* phagosome and evidence that phagosomal maturation is inhibited. *J. Exp. Med.* 181:257–270.
62. Strugill-Koszycki, S., U. Schaible, and D.G. Russel. 1996. Mycobacterium-containing phagosomes are accessible to early endosomes and reflect a transitional state in normal phagosome biogenesis. *EMBO (Eur. Mol. Biol. Organ.) J.* 24: 6960–6968.